Optimisation of CH_4 and CO_2 Conversion and Selectivity of H_2 and CO for the Dry Reforming of Methane by a Microwave Plasma Technique Using a Box-Behnken Design

Nabil Majd Alawi[1,2*], Ahmed Barifcani[1] and Hussein Rasool Abid[1,3]

[1]Western Australian School of Mines: Minerals, Energy & Chemical Engineering, Department of Chemical Engineering, Curtin University, Kent St, Bentley WA 6102, Australia
[2]Petroleum Technology Department, University of Technology, Baghdad, Iraq
[3]Department of Environmental Health, Applied Medical Science College, Karbala University, Iraq
*Corresponding author: n.alawi@postgrad.curtin.edu.au my

Abstract

A microwave plasma was generated by N_2 gas. Synthesis gases (H_2 and CO) were produced by the interaction of CH_4 and CO_2 under plasma conditions at atmospheric pressure. The experimental pilot plant was set-up, and the gases were sampled and analysed by GC/MS. The Box-Behnken design (BBD) method was used to find the optimising conditions based on the experimental results. The response surface methodology (RSM) based on a three-parameter and three-level BBD has been developed to find the effects of independent process parameters, which were represented by the gas flow rates of CH_4, CO_2 and N_2 and their effects on the process performance in terms of CH_4, CO_2 and N_2 conversion and selectivity of H_2 and CO. In this work, four models based on quadratic polynomial regression have been determined to understand the connection between the limits of the feed gas flow rate and the performance of the process. The results show that the most important factor influencing the CO_2, CH_4 and N_2 conversion and the selectivity of H_2 and CO was *CO_2 feed gas flow rate*. At the maximum desirable value of 0.92, the optimum CH_4, CO_2 and N_2 conversion were 84.91%, 44.40% and 3.37%, respectively and the selectivity of H_2 and CO were 51.31% and 61.17%, respectively. This was achieved at a gas feed flow rate of 0.19, 0.38, and 1.49 L min^{-1} for CH_4, CO_2 and N_2, respectively.

Keywords: Box-Behnken Design, Dry Reforming of Methane, Microwave Plasma, Optimisation, Syngas Production

1. Introduction

Due to the increasing demand for energy in recent years, there has been higher usage of fossil fuels. This has led to the release of greenhouse gases such as methane (CH_4) and carbon dioxide (CO_2), causing global warming and subsequent climate change [1]. Consequently, it has become imperative to depend on the modern and economical technologies using greenhouse gases as an alternative source for energy generation (such as synthesis gas production) [2]. Synthesis gas is an environmentally friendly fuel, which is synthesised from greenhouse gases. A mixture of hydrogen and carbon monoxide (H_2 + CO) has been used to produce a wide range of liquid fuels by the Fischer-Tropsch (F-T) process [3]. Additionally, this process can be used to synthesise a wide range of chemicals such as ammonia, ethanol, methanol, alcohol, acetic acid, dimethyl ether, methyl formate, diesel, and gasoline [4]. Methane is the most commonly used gas for synthesis gas production. There are three major methods used to convert methane (CH_4) into synthesis gas, and these include steam reforming of methane (SRM) [5, 6], partial oxidation of methane (POM) [7, 8] and dry reforming of methane (DRM) [9-12] which are described below;

Steam Reforming of Methane (SRM)

The most important technology for high syngas production is SRM. It produces a gas mixture with a high H_2:CO ratio (Eq. (1)) [5]. This technology is an endothermic reaction and needs a high temperature (higher than 700 °C) to activate the reforming reaction [6].

$$CH4 + H2O \rightarrow CO + 3H2 \tag{1}$$

Partial Oxidation of Methane (POM)

POM, which is an exothermic reaction, is more suited to produce synthesis gas [7], as shown in Eq. (2). The advantages of this process include high conversion rates of methane and carbon dioxide, and high selectivity of hydrogen and carbon monoxide, all during a very short residence time [8].

$$CH4 + \frac{1}{2}O_2 \rightarrow CO + 2H2 \tag{2}$$

Dry Reforming of Methane (DRM)

Recently, DRM has been used to produce synthesis gas from greenhouse gases (CH_4 and CO_2). leading to the reduced emissions of these gases to the atmosphere [9, 10], as shown in Eq. (3). DRM yields a lower syngas ratio (H_2/CO=1) [11], suitable for use as feedstock to produce a variety of liquid hydrocarbons via the F-T process [12, 13].

$$CH4 + CO2 \rightarrow 2CO + 2H2 \tag{3}$$

$$CO + 2.15H_2 \rightarrow HC + H_2O \tag{4}$$

Plasma dry reforming of methane technology is considered the best way to convert CO_2 and CH_4 to synthesis gas [14]. Plasma, the fourth state of matter, is a partially ionised gas mixture consisting of ions, atoms, electrons, molecules, free radicals, neutral by-products, and photons [15]. Generally, the plasma process is divided into two main methods; the first is cold plasma (non-thermal plasma) discharge including dielectric barrier discharge (DBD), corona discharge (CD), atmospheric pressure glow discharge (APGD), gliding arc discharge (GAD), microwave discharge (MWD) and spark discharge [16]. The second is thermal plasma including direct current (DC), alternating current (AC) arc torch and radio frequency (RF) [17, 18].

In the nitrogen-plasma process, CO_2 and CH_4 conversion, selectivities and yields of H_2 and CO and H_2/CO ratio are affected by many factors such as feed gas flow rate, CO_2:CH_4 ratio, reactor design, residence time, and discharge power [19]. Several authors [15, 1 and 20] have proved that the effect of feed gas flow rates of CO_2, CH_4, and N_2 is an effective factor in the performance of the plasma process. Firstly, Cleiren, Emelie, et al. [15] reported that the feed flow rate affects the conversion, selectivity, yield, and syngas (H_2/CO) ratio. They found that an increasing CH_4 flow rate leads to a decrease in the conversions of CO_2 and CH_4, selectivities, and yields of H_2 and CO. Secondly, Khoja, Asif Hussain et al. [1] have pointed out that the CO_2:CH_4 ratio affects the plasma stability and performance of the process. They noticed that the CH_4 and N_2 conversion, as well as the CO selectivity increase with increasing CO_2 flow rate, while CO_2 conversion, H_2 selectivity, H_2 and CO yields and H_2/CO ratio all decreased. Finally, Serrano-Lotina, A., and L. Daza [20] found that the conversion of CO_2 and CH_4, selectivity, yield of H_2 and CO, and H_2/CO ratio did not change with increasing N_2 flow rate. Pakhare and Spivey [21] pointed out that the ratio of CO_2/CH_4 affects the plasma stability and the process performance. They found that the CH_4 and N_2 conversion, along with the CO selectivity increase with increasing CO_2/CH_4 ratio, while the CO_2 conversion, H_2 selectivity, H_2 and CO yields and H_2/CO ratio all decreased. Adris et al. [22] concluded that the reactor design affects the plasma stability and process performance. Ashcroft et al. [23] reported that the CO_2, CH_4 and N_2 conversions, H_2 and CO selectivities and yields and H_2/CO ratio decrease with increased residence time. Zhang, A. J. et al. [24] and Jiang, T. et al. [25] reported that the discharge power affects the plasma stability and process performance. They found that the conversions of CO_2, CH_4 and N_2, CO selectivity and H_2, CO yields increase, while H_2 selectivity and H_2/CO ratio decrease with increased power.

The influences of these parameters have not independently affected each other; therefore their interactions must be taken into consideration. Identifying the optimum performance of the plasma process using standard experiments is time-consuming and costly due to the need for multiple experiments under different test conditions [26]. To reduce the difficulty in determining the optimum performance of the plasma process, previous studies have used the chemical model [27-37]. It has been found that the chemical model is useful in determining the optimum value for output responses. This model requires a significantly lower number of experiments compared to using a traditional method [27]. The design of experiments (DoE) can be classified into a two main types Box-Behnken factorial design, and Taguchi methods [28]. The ability to use more than one input factor is a significant advantage of DoE. The most used methodology in DoE is the response surface methodology (RSM) [29]. This facility assumes that various input variables and output responses to be connected. In this way, the impact of single variables and their interactions on each response is more easily understood via 3D and contour interpretations [30]. Two design methods, in response to the surface methodology, have been used to determine the optimisation of the plasma process via the central composite design (CCD) and Box-Behnken design (BBD)methods [31]. Fewer experiments are necessary when using the BBD method, making this a more efficient choice than the CCD method [32]. During the 1950s, Box and collaborators developed the response surface methodology (RSM) [33]. RSM is based on many mathematical and statistical techniques which fit a polynomial equation that depends on the experimental data. [34].

Nitrogen is diatomic gas therefore it is usually used for generating a high energy plasma flame through the dissociation and ionization process [16, 38-45]. However, the discussion about N_2 conversion is rare. One of the more interesting findings that emerged from this study is that N_2 can be converted but only in small percentage approximately 3%. Although, the nitrogen gas is considered as an inert gas, and it has a triple strongest bond (N≡N) [46]. However, it exhibited a conversion ability in the present work. The conversion of nitrogen could be attributed into the high temperature inside the plasma reactor and due to the high energy from the microwave. There is another way to generate the plasma from nitrogen by using eclectic-induced reactions. The plasma induced by electron beam has an energy much higher than the energy needed for ionization and dissociation [47-50].

The temperature inside the plasma reactor is usually above 1600 °C, which is enough to breakdown the triple bonds of nitrogen. Then, nitrogen is possible to consider, as some of this amount may be contributed to produce ammonia and cyanide as a side reaction [43, 51].

$$N_2 + 3H_2 \rightarrow 2NH_3 \quad (5)$$

$$N_2 + CO \rightarrow CN + NO \quad (6)$$

$$CN + H_2 \rightarrow HCN + H \quad (7)$$

The use of the DoE method to optimise the plasma chemical reactions in the microwave is still limited. Therefore, this work focuses on the investigation and optimisation the effect of the different feed gas flow rates upon the CH_4, CO_2 and N_2 conversions and selectivities of H_2 and CO to determine which gas is most significant in terms of the process performance. The Box-Behnken design was employed to design the experiments using RSM. In addition, the impact of different process parameters and their interaction on CH_4, CO_2 and N_2 conversions and selectivities of H_2 and CO are investigated and discussed.

2. Experimental Work

2.1. Experimental Design

Figure 1 shows the schematic diagram of the experimental set up for syngas production by plasma generation. It consists of six essential units:- gas cylinders, mass flow controllers (MFC Alicat Scientific, MCS-Series), gas mixer, plasma reactor (microwave generator [power supply SM1150x and magnetron GA4313] and quartz glass tube), water cooling system, gas sampling unit and gas chromatography/mass spectrometry unit (GS/MSD). More specifically, CH_4 (99.99%), CO_2 (99.99%) and N_2 (99.99%) were supplied to experiment while the flowing of gasses were controlled by the mass flow controllers. After that, the gases were mixed by a gas mixer to achieve the desired composition before entering the plasma reactor. Inside the plasma reactor, the plasma flame was generated by nitrogen gas to provide the condition of gas reaction. The thermocouples of type k were located at different locations in all parts of the experimental apparatus to observe and control the temperatures during the reaction. The gas sample was first drawn by syringe then injected into the GC detector. The cooler trap was set up outside the plasma reactor to distinguish the produced gases from water which may be produced as a side product.

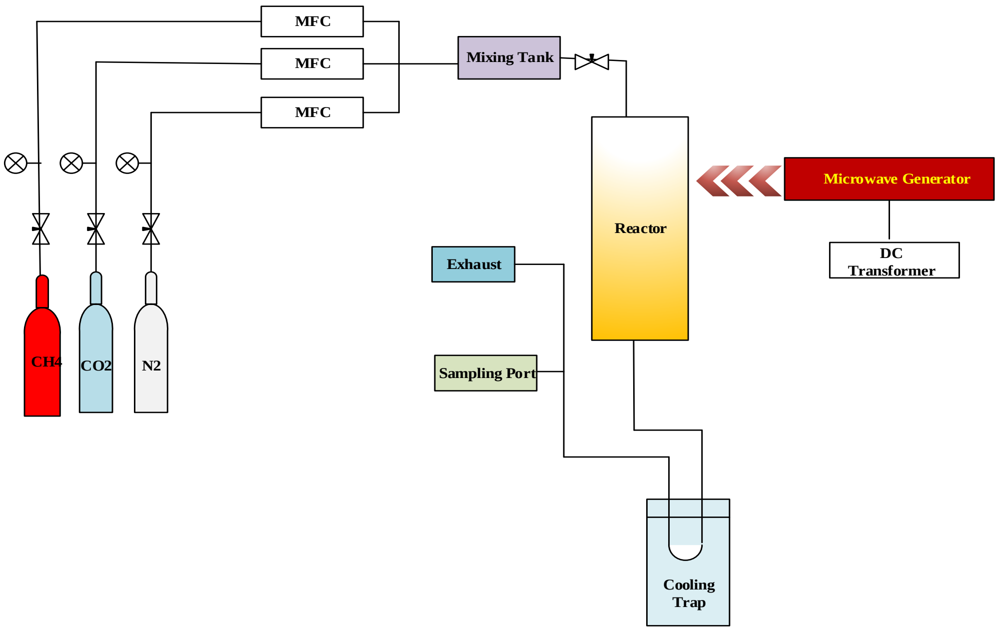

Fig 1. Schematics Flow Diagram of the Experimental Process

2.2. Gas Analysis

The sampled gas was analysed by GC which is gas chromatography combined online with a mass selective detector (MSD). GC can separate and identify the gases such as CH_4, CO_2, H_2, CO, and N_2 by using the thermal conductivity detector (TCD) detector. On the other hand, the structure information was determined by using the MSD. The conversion of CH_4 and CO_2 (C); and the selectivity of H_2 and CO (Y) are presented by the following equations:

$$C\ CH_4(\%) = \frac{\text{moles of } CH_4 \text{ converted}}{\text{moles of } CH_4 \text{ introduced}} \times 100 \tag{8}$$

$$C\ CO_2(\%) = \frac{\text{moles of } CO_2 \text{ converted}}{\text{moles of } CO_2 \text{ introduced}} \times 100 \tag{9}$$

$$C\ N_2(\%) = \frac{\text{moles converted of x}}{\text{moles introduced of x}} \times 100 \tag{10}$$

$$Y\ H_2\ (\%) = \frac{\text{moles of H2 produced}}{2 \times \text{moles of CH4 converted}} \times 100 \tag{11}$$

$$Y\ CO\ (\%) = \frac{\text{moles of CO produced}}{[\text{moles of CH4 + moles of CO2}] \text{ converted}} \times 100 \tag{12}$$

Where x indicates one of the chemicals from N_2 conversion.

2.3. Approximate Model Function

The response surface method (RSM) is a set of mathematical and statistical tool that is helpful for the modelling and analysis of problems [32]. RSM refers to a function of independent parameters described as [35]:

$$y = f(x_1, x_2, x_3, \dots, xi) \quad (13)$$

Where y is the response variable, f is the response function, and x_1, x_2, …, x_i are the independent input parameters. RSM is a very beneficial and helpful method to control variables in experiments and optimise the operating parameters with as few errors as possible [36]. The relationship between the independent parameters and the response surface is essential because it gives the real functional relationship. Additionally, the second-order model is used in RMS [37].

In this study, three factors in the three-level Box-Behnken design (BBD) were utilised to investigate the interaction impact among these factors on the performance process of CO_2 and CH_4 conversions and H_2 and CO **yields**. In this work, the flow rates of CH_4 (x_1), CO_2 (x_2), and N_2 (x_3) have been identified as the three independent variables affecting the conversions of CH_4, CO_2 and N_2 and the selectivities of H_2 and CO. Therefore, they were selected as the input parameters for the BBD, while conversions of CH_4 (Y_1), CO_2 (Y_2) and N_2 (Y_3), and selectivities of H_2 (Y_4) and CO (Y_5) are identified as responses. Either independent process variable contains three different levels, which are coded as low (-1), centre (0) and high (+1), as shown in Table 1.

Table 1. Experimental range and levels of the independent input variables in the Box-Behnken design.

Independent Variables	Symbols	Level and Range		
		Low [-1]	Centre [0]	High [+1]
CH_4 [L/min.]	x_1	0.1	0.2	0.3
CO_2 [L/min.]	x_2	0.2	0.4	0.6
N_2 [L/min.]	x_3	1.4	1.5	1.6

The BBD, the regression (quadratic) model describes the relationship between the input process variables and each response. The quadratic model used to predict the optimal values is presented by the following equation [52]:

$$Y = \beta_0 + \sum_{i=1}^{k} \beta_i x_i + \sum_{i}^{k} \beta_{ii} x_{ii^2} + \sum_{i=1}^{k-1} \sum_{j=i+1}^{k} \beta_{ij} x_i x_j \quad (14)$$

where Y is the response; β_0 is the constant coefficient; β_i is the coefficient for linear; x_i is the initial input parameters; β_{ii} (i = 1, 2, …, k) are the quadratic coefficients, and β_{ij} (i = 1, 2, …, k; j = 1, 2, k) are the coefficients that represent the interactions of x_i and x_j [53]. The reaction performance can be predicted at different process conditions by this model [54].

Analysis of variance (ANOVA) is used to estimate the indication of adequacy and modelling fitting. Response surfaces were generated by JMP statistical discovery™ software from SAS (version 13.1.0), which was used in the regression analysis and to plot the contour and 3-dimensional surface figures. The multiple coefficients of determination (R^2) values were found by the variance of variables and identified the interaction between the parameters within the particular experimental boundary conditions. The interaction between parameters was obtained by using the model equation to determine the optimum response values.

3. Results and Discussion

In this research, H_2 and CO were found to be the main two gas products that result from the CH_4 and CO_2 conversion. The CO_2:CH_4 molar ratio was kept at 2:1, and the microwave power at 700 W. The conversions of CH_4, CO_2 and N_2 were within the ranges of (94.67-79.35%), (65.24-44.82%) and (11.67-3.22%), respectively. Meanwhile, the selectivities of H_2 and CO were (70.85-50.12%) and (75.32-58.42%), respectively. The conversion of CH_4 was always higher than those of CO_2 and N_2. That can be attributed to the nature of the gas molecules, where these gases have a different molecular structure with different chemical bonds. Methane has covalent bonds, and a large amount of energy may be released when they are broken [55]. Additionally, the rate of dissociation of methane molecule depends on the initial supplied energy. On the other hand, the rate of thermal dissociation of CO_2 was lower due to its dependence on both temperature and the initial concentrations of CO_2 [56] which adversely affect the conversion of CO_2. N_2 gas is dissociated due to applied microwave energy, as shown in Eq. (15) which produces the plasma flame. Moreover, the produced N atoms may adhere to the wall of the quartz tube and lead to recombination of nitrogen atoms again, as shown in Eq. (16) [57]. This mechanism leads to the reproduction of N_2 gas and reduces the conversion rate in the product.

$$\mathrm{N_2} \rightarrow \mathrm{N} + \mathrm{N} \tag{15}$$

$$\mathrm{N} + \mathrm{N} + \mathrm{wall} \rightarrow \mathrm{N_2} \tag{16}$$

3.1 Analysis of Multiple Regressions

Fifteen experimental samples were selected randomly for the BBD, including triplicate experimental runs, as shown in Table 2. The real relationships between the input and output values are presented in four equations based on the DoE analysis. The CH_4, CO_2 and N_2 conversion (Y_1, Y_2 and Y_3), and the selectivity of H_2 and CO (Y_4, Y_5) are presented in Equation (17)-(21).

$$Y_1 = 77.80 + 6.41x_1 - 32.32x_2 + 2.63x_3 + 0.64x_1x_2 + 7.13x_1x_3 - 0.91x_2x_3 - 9.84x_1^2 - 36.08x_2^2 - 8.93x_3^2 \tag{17}$$

$$Y_2 = 43.38 - 2.43x_1 - 12.19x_2 - 0.84x_3 + 1.28x_1x_2 - 0.32x_1x_3 - 0.85x_2x_3 - 4.35x_1^2 - 25.54x_2^2 - 6.94x_3^2 \tag{18}$$

$$Y_3 = 3.08 + 0.04x_1 - 1.33x_2 - 0.04x_3 + 0.04x_1x_2 - 0.08x_1x_3 + 0.065x_2x_3 - 0.26x_1^2 - 1.45x_2^2 - 0.32x_3^2 \tag{19}$$

$$Y_4 = 48.78 + 0.58x_1 - 16.24x_2 + 0.26x_3 + 0.107x_1x_2 + 1.005x_1x_3 - 0.38x_2x_3 - 5.03x_1^2 - 25.75x_2^2 - 8.54x_3^2 \quad (20)$$

$$Y_5 = 57.35 + 0.23x_1 - 21.1x_2 + 0.05x_3 + 0.02x_1x_2 + 0.28x_1x_3 - 0.38x_2x_3 - 6.05x_1^2 - 29.09x_2^2 - 8.26x_3^2 \quad (21)$$

ANOVAs were used to determine the significance and adequacy of the quadratic models (Tables 2-7). The coefficient of determination (R^2) of the regression equations for the process parameters (CH_4, CO_2 and N_2 conversions) and process performances (H_2 and CO selectivities) were 0.97, 0.99, 0.97, 0.99 and 0.99, respectively. The relationship between the variables and responses is described by the second order equation and this shows a good agreement between the experimental and predicted values because R^2 is close to 1, as shown in Figure 2. These results indicate that the quadratic models are statistically significant also able to predict and optimise the CH_4, CO_2 and N_2 conversions and yields of H_2 and CO due to minimum error bar, as shown in Figure 2. Moreover, leverage residuals values were 47.74, 23.73, 1.2, 27.81 and 34.2 for the conversions CH_4, CO_2, N_2, H_2 and CO which measures of how of the variables have a significant effect on the process performance. As shown in Figure 2, CO_2 is identified as a significant factor because the more of values were pass close to the leverage residuals line.

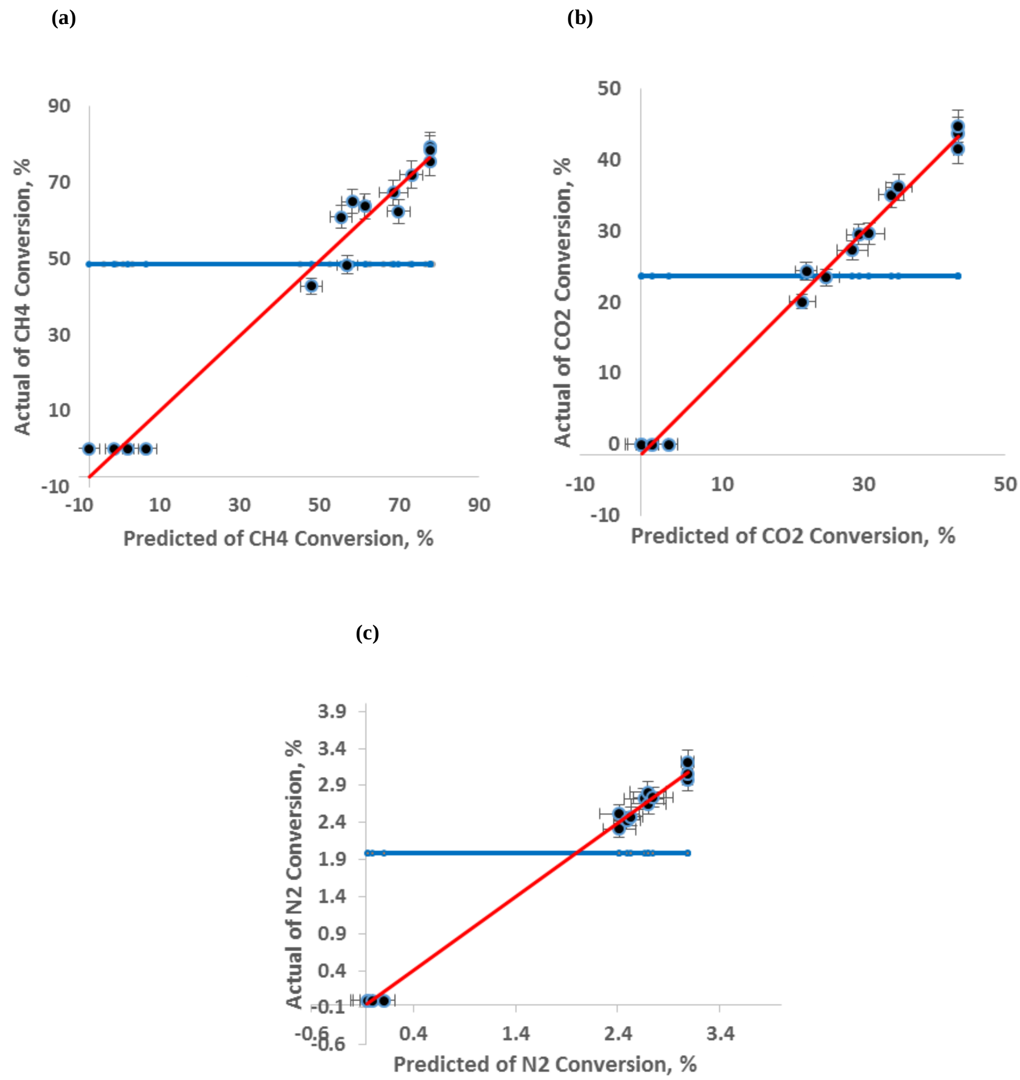

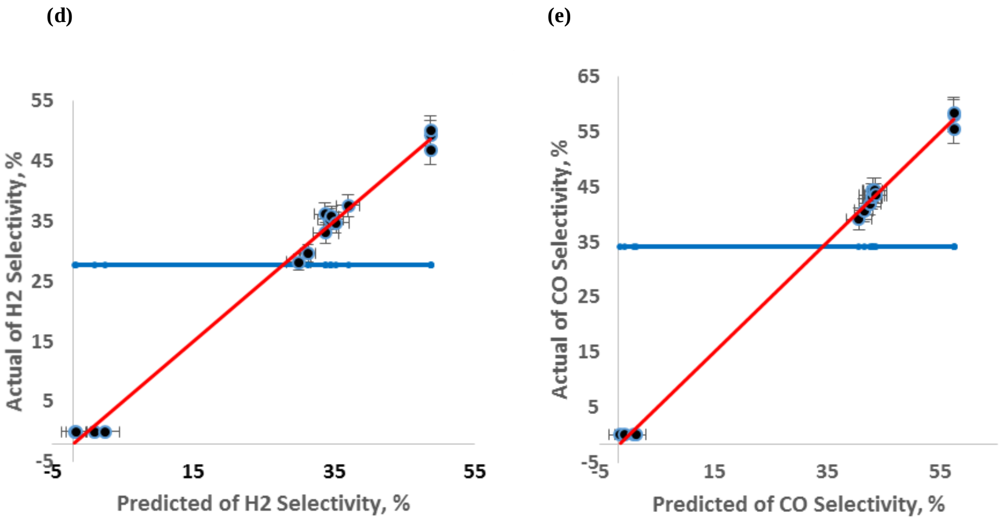

Fig 2. Comparison between actual and predicted values; (a) Conversion of CH_4; (b) Conversion of CO_2; (c) Conversion of N_2; (d) Selectivity of H_2; (e) Selectivity of CO [(•) experimental points, (···) confidence bands > (95%), (–) fit line, Eqs. (17)-(21), (–) mean of the Y leverage residuals].

3.2 Effects of Plasma Process Parameters

3.2.1 CH_4, CO_2 and N_2 Conversions

The coefficient (β), standard error (ST), the squares sum (SS), the degree of freedom (DF), f-values and p-values are created by ANOVA, as presented in Table 3. The importance of this factor is indicated by its f-value and the p-value which indicates the level of significance of the parameter. The influence is considered significant on the performance of process if the p-value of a term (individual parameter x_i or interaction of two parameters x_ix_j) is below 0.05, while it is not significant if the p-value is above 0.05.

In the CH_4, CO_2 and N_2 conversion, the variables x_2, x_1^2, x_2^2 and x_3^2 are identified as significant factors ($p<0.005$), while the variables x_2, x_1^2, x_2^2 and x_3^2 are not significant ($p>0.005$), as shown in Tables 3-7. These results suggest that the term of CO_2 is the most significant impact on conversions of CH_4 and CO_2 compared to the other parameters because it has the highest f-value among the CH_4, CO_2 and N_2 conversion which are 96.78, 200.87 and 745.96, respectively (shown in Tables 3-5). The 3D response surface and 2 D contour lines are based on Equations (9)-(11) plots in Figures 3-5, respectively with one independent factor kept at a constant level (coded zero level), while the other two factors were changed within the experimental ranges.

These figures show the effects of CH_4 and CO_2 feed flow rates on CH_4 and CO_2 conversions at a CO_2:CH_4 ratio of 2:1 and the microwave power at 700 W. Figures 3 and 4 show that the responses enhanced as corresponding factors (flow rate of CH_4, CO_2 and N_2) peaked, and after that, they decreased when it (the corresponding factor) increased to more than 0.19, 0.38 and 1.49 L min^{-1}, respectively. Figure 3a indicated that the CH_4 conversion increased rapidly when the CH_4, CO_2 and N_2 flow rates ranged from 0.1 to 0.19, 0.2 to 0.38 and 1.4 to 1.49 L min^{-1} , respectively, and then declined when the flow rate increased to greater than 0.19, 0.38 and 1.49 L min^{-1}, respectively. This is because the reduction in the conversion of CH_4, CO_2 and N_2 could be related to the residence time of gases in the microwave discharge zone, and it is reduced with the increase in gas feed flow rate; this led to the shorter treatment time [21].

Maximum CH_4, CO_2 and N_2 conversions of 84.91%, 44.40% and 3.37%, respectively were achieved at the highest gas feed flow rates of 0.19, 0.38 and 1.49 L min^{-1} for CH_4, CO_2 and N_2, respectively. The conversion of CH_4 and CO_2 decreased with increasing the feed flow rates for CH_4, CO_2 and N_2 from 0.05 to 0.19, 0.1 to 0.38 and 0.3 to 1.49 L min^{-1}, respectively. This is due to the reduction in conversions of CH_4, CO_2 and N_2 which could be related to the residence time in the microwave discharge zone. Moreover, its value was reduced with the increasing of gas feed flow rate, which led to the shorter treatment time [20], as plotted in Figures 3, 4 and 5(b, d, and f). These results indicate that the interactions of the conversion of CH_4 (0.1083, 0.4590, 0.8950, 0.1852 and 0.8513) as shown in Table 3 i.e., the terms x_1, x_3, x_1x_2, x_1x_3 and x_2x_3 are not significant. Likewise, the interaction of the two parameters on the plasma process is not considered significant on the CO_2 and N_2 conversion as shown by the high p-values (0.0365, 0.3692, 0.3401, 0.8015 and 0.5160) and (0.4243, 0.3207, 0.5879, 0.2994 and 0.3902), of the terms x_1, x_3, x_1x_2, x_1x_3 and x_2x_3, respectively, as listed in Tables 4 and 5.

(a) **(b)**

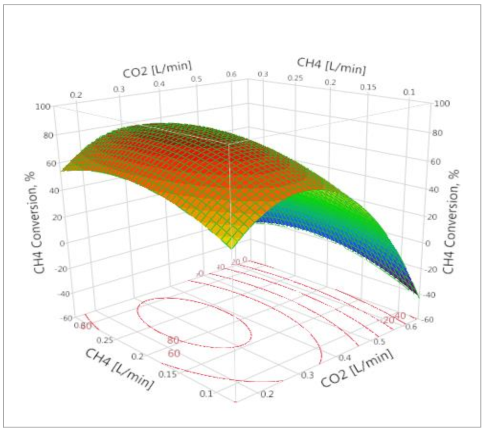

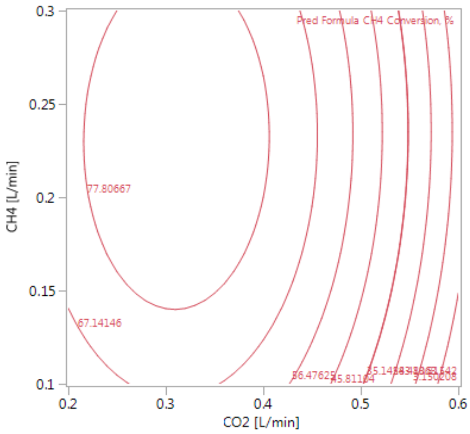

(c) **(d)**

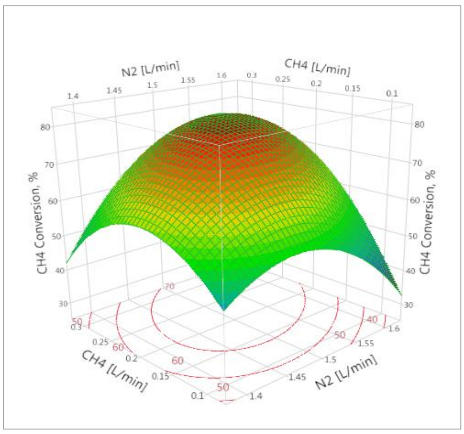

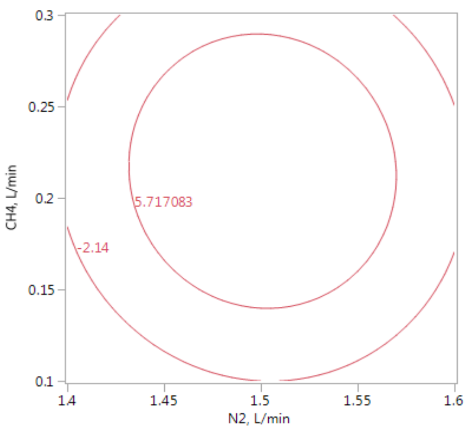

(e) **(f)**

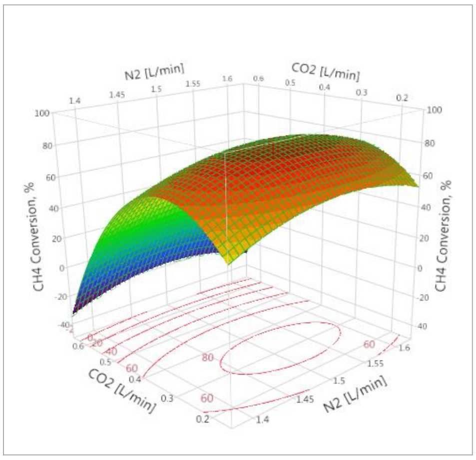

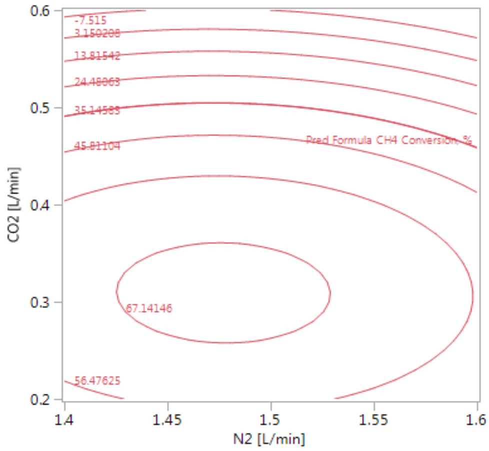

Fig. 3. Effect of feed gas flow rates and their interaction on CH_4 conversion at a CO_2:CH_4 ratio of 2:1 and microwave plasma of 700 W (a, c, and e) three-dimensional surface plot; (b, d, and f) projected contour plot.

(a) **(b)**

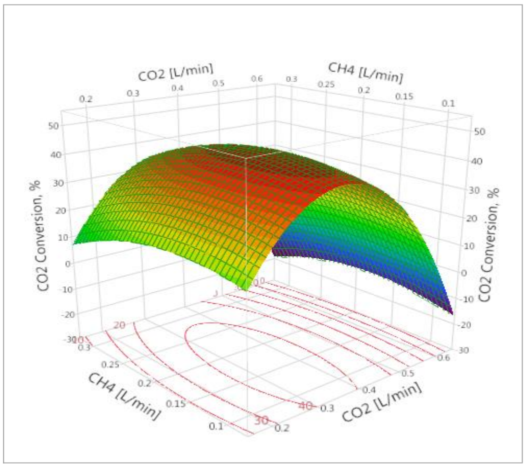

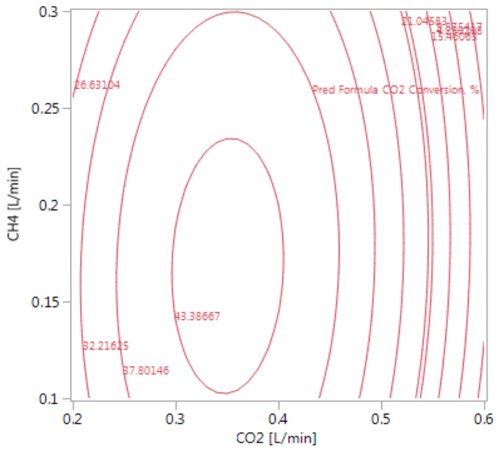

(c) **(d)**

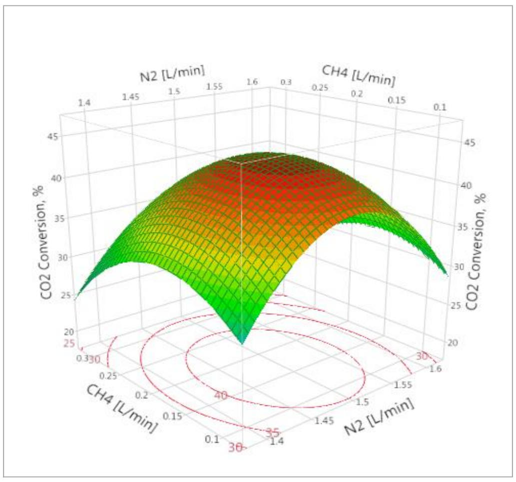

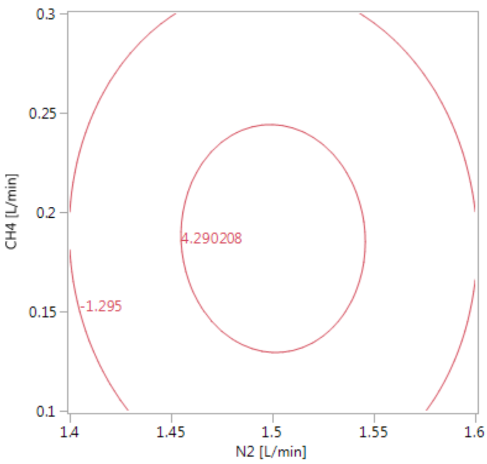

(e) **(f)**

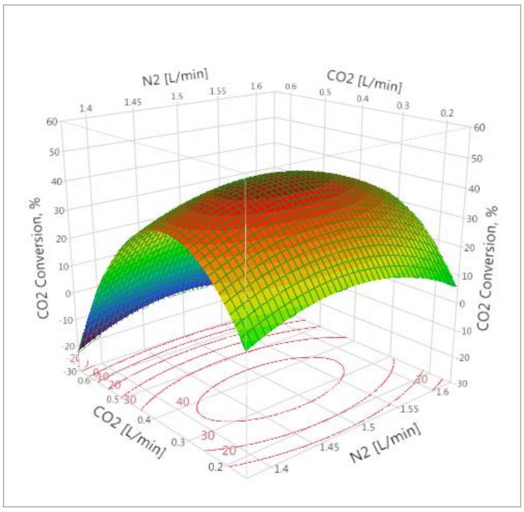

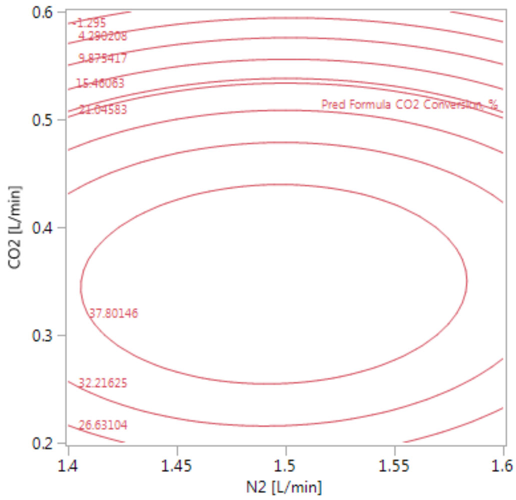

Fig. 4. Effect of feed gas flow rates and their interaction on CO_2 conversion at a CO_2:CH_4 ratio of 2:1 and microwave plasma of 700 W (a, c and e) three-dimensional surface plot; (b, d, and f) projected contour plot.

(a) **(b)**

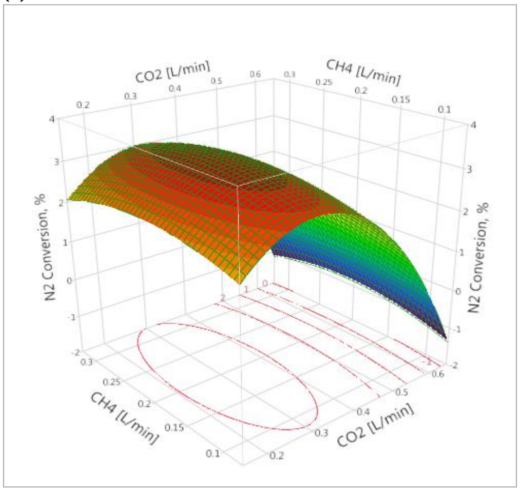

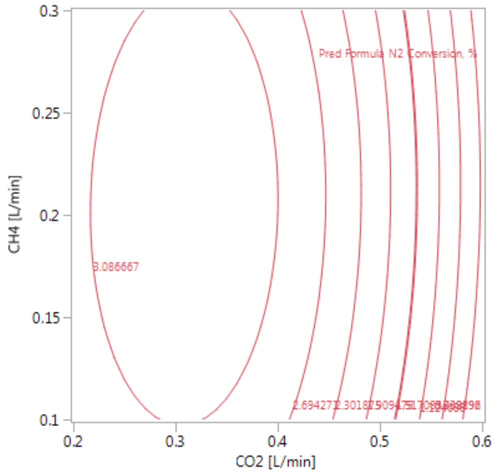

(c) **(d)**

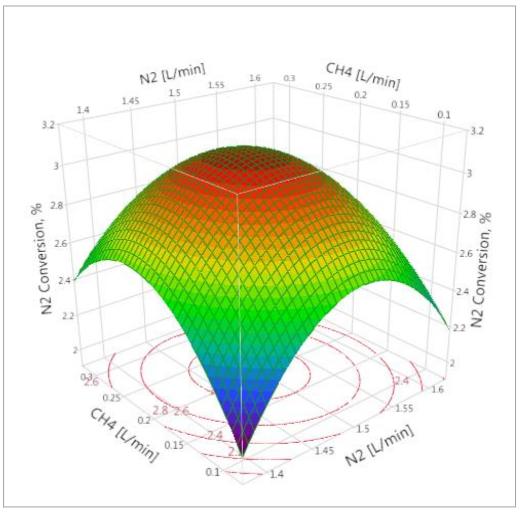

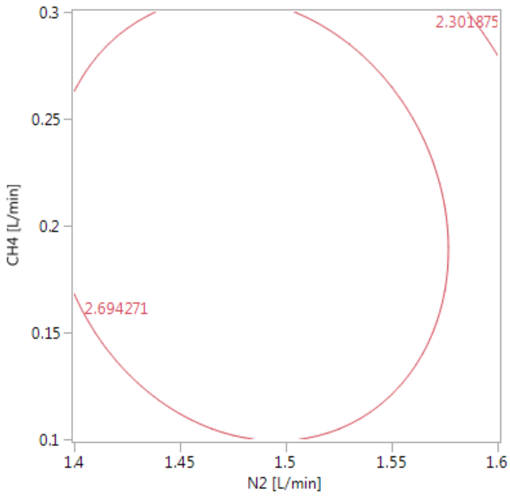

(e) **(f)**

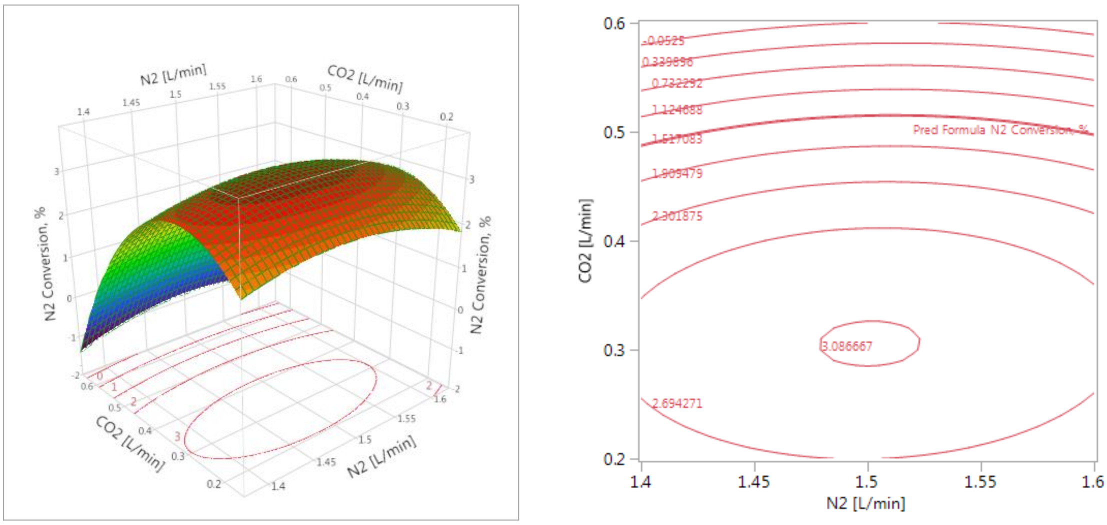

Fig. 5. Effect of feed gas flow rates and their interaction on N_2 conversion at a CO_2:CH_4 ratio of 2:1 and microwave plasma of 700 W (a, c and e) three-dimensional surface plot; (b, d, and f) projected contour plot.

3.2.3 H_2 and CO Selectivity

The ANOVA results for the quadratic model are shown in Tables 6 and 7. In H_2 and CO selectivity, the terms x_2, x_1^2, x_2^2 and x_3^2 are identified as significant, while the terms x_1, x_3, x_1x_2, x_1x_3 and x_2x_3 are not considered significant. These results indicate that the CO_2 term is more important than the interactions between various parameters in term of selectivities of H_2 and CO. As shown in Tables 6 and 7, the CO_2 flow rate has the highest F-value while it is 307.7060 and 1141.848 for CH_4 and CO respectively, so it reflected the most significant effect on selectivities of H_2 and CO. The highest H_2 and CO selectivities of 51.31% and 61.17% were achieved at the optimal gas feed flow rate of CH_4 (0.19 L min^{-1}), CO_2 (0.38 L min^{-1}) and N_2 (1.49 L min^{-1}), respectively. The effect of different factors and their interaction on selectivities of H_2 and CO are shown by the 3D response surface plots and 2 D contour lines and represented by Eqs. (13) and **(**14), as shown in Figures 6 and 7. The reduction in selectivities of H_2 and CO could be related to the consumed time for gases inside the microwave discharge zone, which was reduced with increasing flow rates of the gases [58], as shown in Figures 6 and 7(b, d, and f).

This behaviour is similar to that reported previously [38, 40-43, 45, 59, 60]; these studies have shown that the conversions of CH_4 and CO_2 and selectivities of H_2 and CO were decreased with increasing gas feed flow rates. The interactions between the two parameters on the selectivities of H_2 and CO are not considered significant as illustrated in Tables 6 and 7 respectively. This was confirmed when high p-values (p-values for x_1, x_3, x_1x_2, x_1x_3 and x_2x_3) for H_2 and CO selectivity were obtained. It was 0.5561, 0.7881, 0.9378, 0.4774 and 0.7833 for H_2 and 0.7263, 0.9378, 0.9828, 0.7579 and 0.6810 for CO.

(a) **(b)**

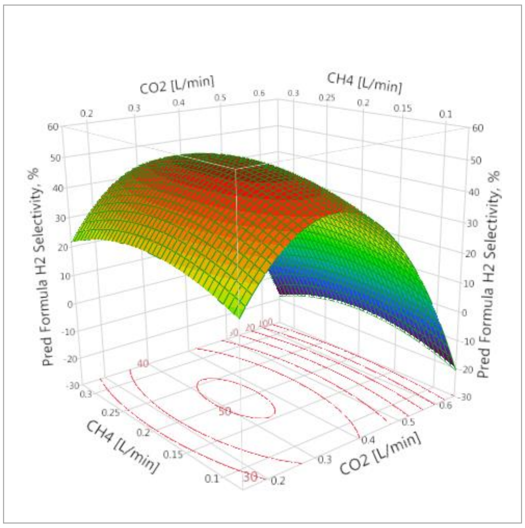
CO2 [L/min]
CH4 [L/min]
Pred Formula H2 Selectivity, %
CH4 [L/min]
CO2 [L/min]

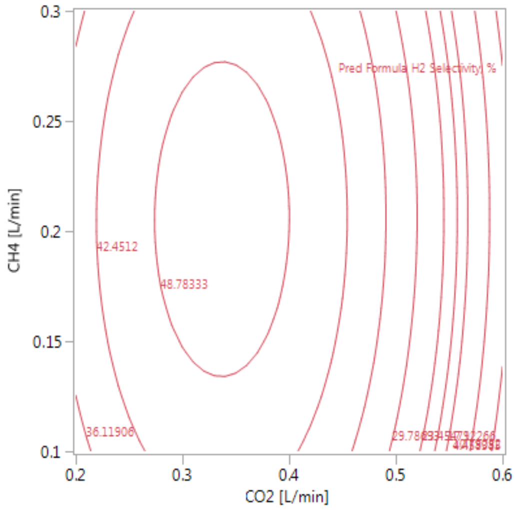
Pred Formula H2 Selectivity, %
42.4512
48.78333
36.11906
CH4 [L/min]
CO2 [L/min]

(c)

(d)

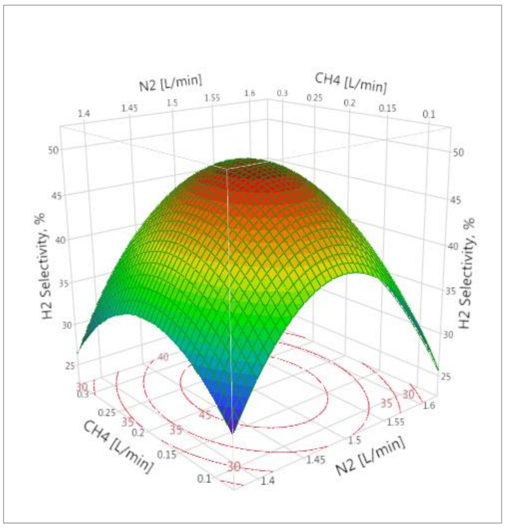
N2 [L/min]
CH4 [L/min]
H2 Selectivity, %
CH4 [L/min]
N2 [L/min]

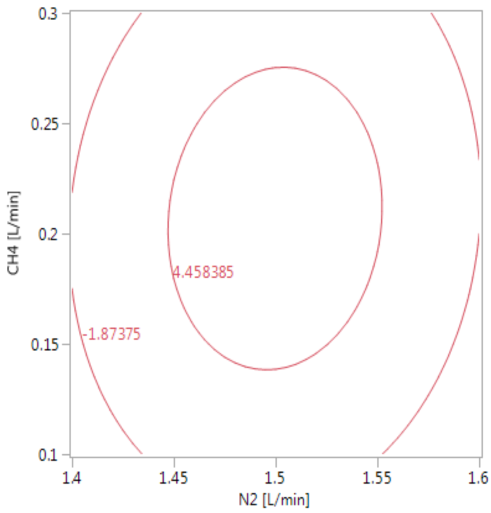
4.458385
-1.87375
CH4 [L/min]
N2 [L/min]

(e)

(f)

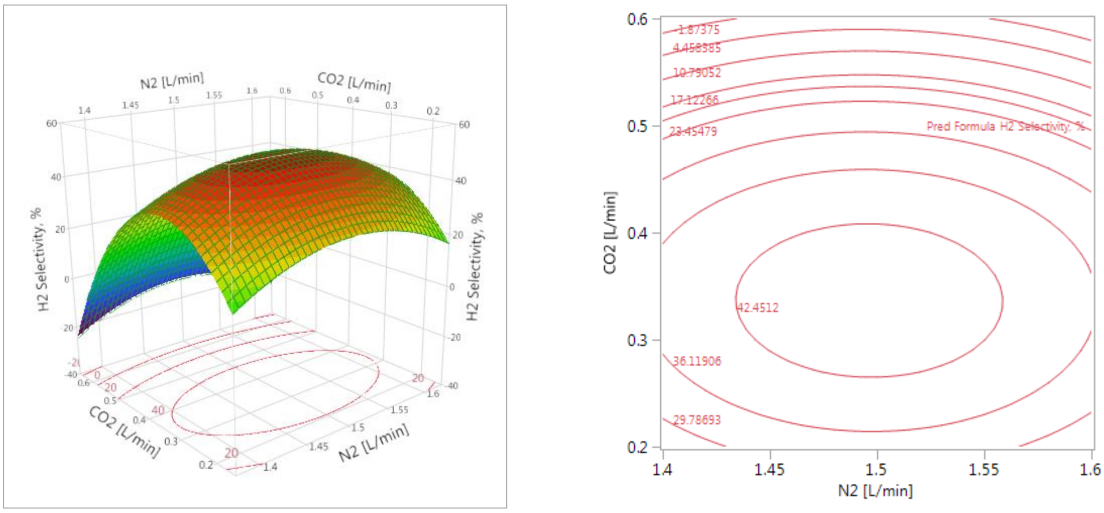

Fig. 6. Effect of feed gas flow rates and their interaction on H_2 selectivity at a CO_2:CH_4 ratio of 2:1 and microwave plasma of 700 W (a, c, and e) three-dimensional surface plot; (b, d, and f) projected contour plot.

(a) **(b)**

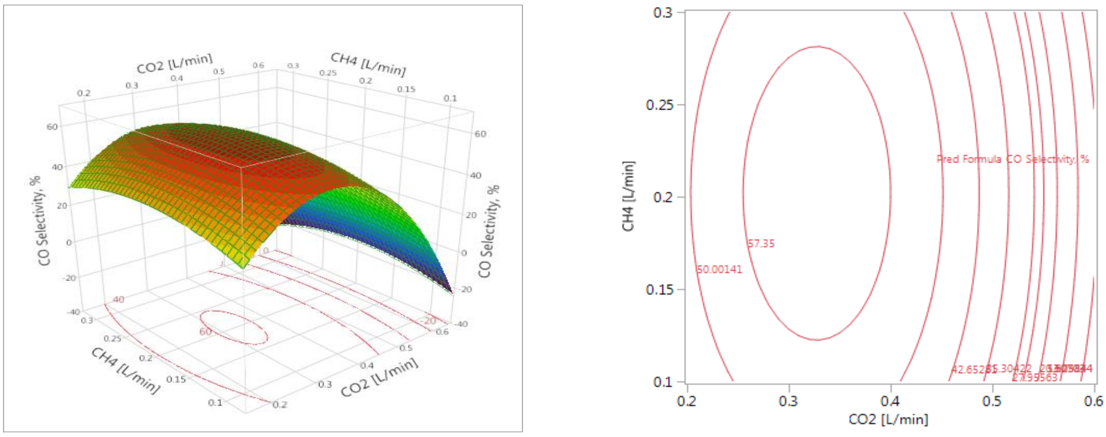

(c) **(d)**

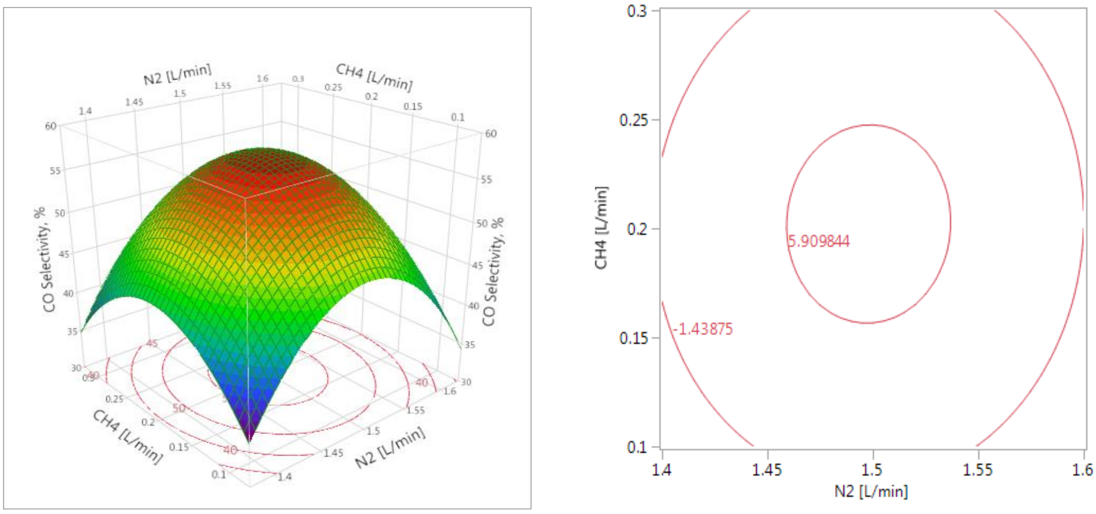

(e) **(f)**

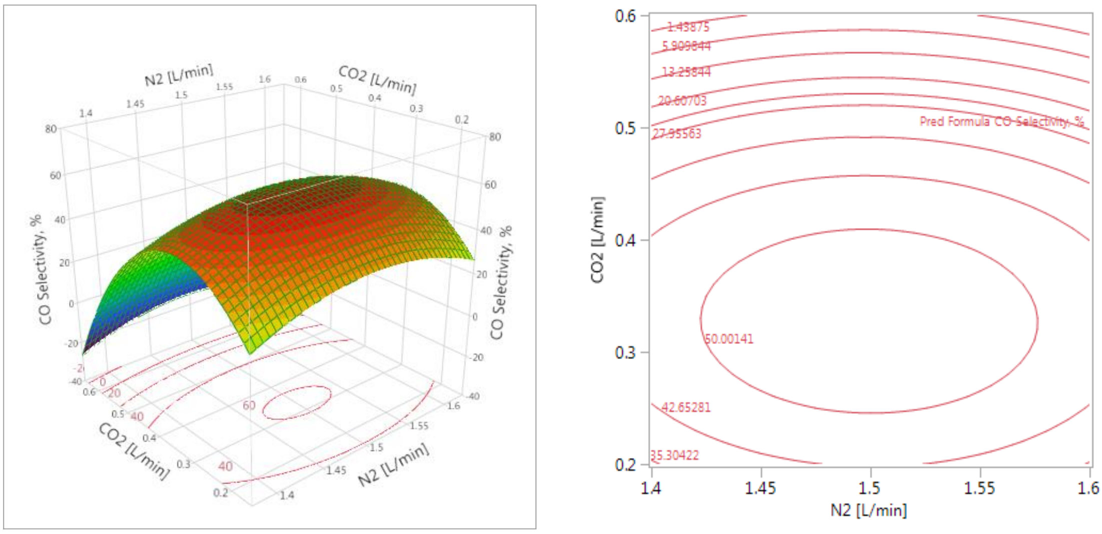

Fig. 7. Effect of feed gas flow rates and their interaction on CO selectivity at a CO_2:CH_4 ratio of 2:1 and microwave plasma of 700 W (a, c and e) three-dimensional surface plot; (b, d and f) projected contour plot.

4. Desirability and Optimum conditions

The optimum operating conditions were determined for several input variables, which led to obtaining the desirable output response values. Desirability Function (DF) method is used to prove the optimal approaches of multiple responses. Also, the values of DF are dimensionless and ranged from zero to one (zero means the unacceptable response value while one represents gaining the goal) [61]

In this research, the maximised desirability flow rates of CO_2, CH_4 and N_2 is 0.92. This value for the desirability gives strong supporting to the fitting model. The optimal experimental conditions were achieved at CH_4 = 0.19 L/min, CO_2 = 0.38 L/min and N_2 =1.49 L/min, respectively. The validity of the equations of the model (Eqs. 17-21) is good with a reasonable error, as shown in Table 8.

Therefore, the balance between conversions (CH_4, CO_2 and N_2) and selectivities (H_2 and CO) is important in the development of an active plasma process for CH_4 and CO_2 conversions. Thus, the performance of the plasma process generally depends on a wide range of operating conditions and especially on the flow rates. It is necessary and fundamental for optimising the performance plasma process with multiple inputs and multiple responses. This study aims to optimise the process to find the plasma process variables (various parameters) that jointly optimise the CH_4, CO_2 and N_2 conversions and selectivities of H_2 and CO (various responses).

Table 9 summarises the results of conversions and selectivities in the previous studies compared with those in this work. It has been demonstrated that this study obtained acceptable results amongst others. All previous reports were done a different operating conditions which are higher than those used in this study including the flow rate, CO2/CH4 ratio and microwave power. In this research, the total feed flow rate of 2.04 L min^{-1}, CO2/CH4 ratio of 2/1 and microwave power of 700 W were used for producing microwave plasma with a good performance. The conversions of CH_4, CO_2 and N_2 were 84.91%, 44.40% and 3.37%, in sequence while the selectivities of H_2 and CO were 51.31% and 61.17%, respectively. Hwang [40] claimed that the highest selectivities can be achieved at high feed flow rate and input power. Although they used an input power of 1000 W and total flow rate of 20 L min^{-1} which were higher than those in the present work, the conversion in this study is greater than their conversion. In addition, Long, Shang [38] found that the conversions of CH_4 and CO_2 and selectivities of H_2 and CO were changed with increasing flow rate also the optimum flow rate and input power were 16.667 L min^{-1} and 770 W respectively. However, as shown in Table 9, the present conversions were higher than their conversions. Moreover, Chun and Lim [62] reported that the microwave discharge affected the stability of plasma and the process performance. It can be shown in Table 9, that their conversions of CH_4 and CO_2 at a low total flow rate (2.25 ml. min^{-1})and a high microwave energy(2000W) was lower than the conversions of CH_2 and CO_2 in this study.

Furthermore, Fidalgo and Menéndez [63] investigated how the flow rate and microwave energy affected the CH_4 and CO_2 conversions and selectivities of H_2 and CO. They claimed that the maximum CH_4 and CO_2 conversions and the selectivities of H_2 can be obtained at high total flow rate of 33.34 L min^{-1} and microwave power of 83000 W. Their results were higher than the present results although they used lower specific energy which was due to using a microwave laboratory pilot plant with CO_2 gas as the plasma generation gas. Eventually, Chun, Hong [64] pointed out that microwave power affected the plasma stability and performance of the process. They noticed that the CH_4 and CO_2 conversions and the H_2 and CO selectivities were improved at the total flow rate of 30 L min^{-1} and the high microwave power of 6000 W. They used feed flow rates and power a higher than this work but the results in term conversions and selectivities were fairly close, as shown in Table 9. It seems that the results of this research are more reliable for conversion of CO_2 and CH_4 and producing CO and H_2 with high selectivities.

Table 2. Actual values of the independent variables with the experimental and predicted values in the Box-Behnken Design

Run order	Actual Values			Response Values, CH_4 Conversion [%]		Response Values, CO_2 Conversion [%]		Response Values, N_2 Conversion [%]		Response Values, H_2 Selectivity [%]		Response Values, CO Selectivity [%]	
	X_1	X_2	X_3	[d]Experimental of CH_4 Conversion	Predicated of CH_4 Conversion	[d]Experimental of CO_2 Conversion	Predicted of CO_2 Conversion	[d]Experimental of N_2 Conversion	Predicted of N_2 Conversion	[d]Experimental of H_2 Selec.	Predicted of H_2 Selec.	[d]Experimental of CO Selec.	Predicted of CO Selec.
1[a]	0.2	0.4	1.5	70.29	72.36	38.65	40.35	2.77	2.87	43.61	45.36	51.75	53.33
2[b]	0.2	0.4	1.5	72.1	72.36	40.71	40.35	2.84	2.87	45.88	45.36	53.92	53.33
3	0.1	0.4	1.6	39.77	44.74	32.69	31.63	2.25	2.31	30.75	31.49	39.04	39.58
4	0.1	0.2	1.5	60.49	54.33	27.47	27.35	2.61	2.51	33.67	31.39	41.33	40.07
5	0.2	0.2	1.6	62.68	63.85	18.69	19.89	2.31	2.35	27.64	29.16	37.91	38.62
6	0.3	0.2	1.5	58.09	65.07	22.71	20.43	2.46	2.52	33.27	32.28	41.26	40.46
7	0.2	0.6	1.6	0	-2.01	0	-1.21	0	-0.08	0	-1.73	0	-1.33
8	0.1	0.4	1.4	44.94	53.11	33.67	32.62	2.14	2.24	32.35	32.88	40.11	40.01
9	0.2	0.6	1.4	0	-1.17	0	-1.21	0	-0.04	0	-1.52	0	-0.71
10	0.3	0.4	1.6	68.81	69.94	25.41	26.48	2.34	2.24	34.99	34.46	40.47	40.55
11[c]	0.2	0.4	1.5	73.79	72.36	41.68	40.35	2.99	2.87	46.61	45.36	54.33	53.33
12	0.1	0.6	1.5	0	-6.98	0	-2.27	0	-0.04	0	-0.98	0	-0.79
13	0.2	0.2	1.4	59.27	57.24	21.85	23.05	2.54	2.55	26.23	27.98	36.47	37.81
14	0.3	0.6	1.5	0	-6.14	0	0.13	0	0.11	0	2.27	0	1.26
15	0.3	0.4	1.4	56.74	51.77	27.59	30.83	2.52	2.66	32.85	34.52	40.46	42.92

[a-c]Replicated experimental runs (Run order 1, 2, and 14); [d]Responses are shown as the means of three replicates with a standard deviation

Table 3. ANOVA results for the quadratic regression model of CH_4 conversion

Model Terms	B[a]	SE[b]	SS[c]	DF[d]	*F*-Value	*P*-Value
Intercept	77.806667	5.366206	-	-	-	-
X_1	6.41625	3.286116	329.3461	1	3.8124	0.1083
X_2	-32.32875	3.286116	8361.1846	1	96.7859	<.0001*
X_3	2.635	3.286116	55.5458	1	0.6430	0.4590
$X_1 X_2$	0.645	4.64727	1.6641	1	0.0193	0.8950
$X_1 X_3$	7.1375	4.64727	203.7756	1	2.3588	0.1852
$X_2 X_3$	-0.9175	4.64727	3.3672	1	0.0390	0.8513
X_1^2	-9.845833	4.837032	357.9339	1	4.1433	0.0974
X_2^2	-36.08583	4.837032	4808.0764	1	55.6564	0.0007*
X_3^2	-8.938333	4.837032	294.9925	1	3.4147	0.1239

R^2, 0.97; [a]Coefficient; [b]Standard error; [c]Sum of Squares; [d]Degrees of freedom; f-values and p-values

Table 4. ANOVA results for the quadratic regression model of CO_2 conversion

Model Terms	B[a]	SE[b]	SS[c]	DF[d]	*F*-Value	*P*-Value
Intercept	43.386667	1.404953	-	-	-	-
X_1	-2.4375	0.860354	47.5312	1	8.0267	0.0365
X_2	-12.19375	0.860354	1189.5003	1	200.8722	<.0001*
X_3	-0.84875	0.860354	5.7630	1	0.9732	0.3692
$X_1 X_2$	1.2825	1.216725	6.5792	1	1.1110	0.3401
$X_1 X_3$	-0.3225	1.216725	0.4160	1	0.0703	0.8015
$X_2 X_3$	0.85	1.216725	2.8900	1	0.4880	0.5160
X_1^2	-4.353333	1.266407	69.9748	1	11.8167	0.0185*
X_2^2	-25.54583	1.266407	1109.5616	1	106.9052	<.0001*
X_3^2	-6.940833	1.266407	177.8775	1	30.0384	0.0028*

R^2, 0.99; [a]Coefficient; [b]Standard error; [c]Sum of Squares; [d]Degrees of freedom; f-values and p-values

Table 5. ANOVA result for the quadratic regression model of N_2 conversion

Model Terms	B[a]	SE[b]	SS[c]	DF[d]	*F*-Value	*P*-Value
Intercept	3.0866667	0.079819	-	-	-	-
X_1	0.0425	0.048879	0.014450	1	0.7560	0.4243
X_2	-1.335	0.048879	14.257800	1	745.9609	<.0001*
X_3	-0.0425	0.048879	0.014450	1	0.7560	0.3207
$X_1 X_2$	0.04	0.069125	0.006400	1	0.3348	0.5879
$X_1 X_3$	-0.08	0.069125	0.025600	1	1.3394	0.2994
$X_2 X_3$	0.065	0.069125	0.016900	1	0.8842	0.3902
X_1^2	-0.265833	0.071948	0.260926	1	13.6515	0.0141*
X_2^2	-1.455833	0.071948	7.825664	1	409.4348	<.0001*
X_3^2	-0.325833	0.071948	0.392003	1	20.5094	0.0062*

R^2, 0.97; [a]Coefficient; [b]Standard error; [c]Sum of Squares; [d]Degrees of freedom; f-values and p-values

Table 6. ANOVA result for the quadratic regression model of H_2 selectivity

Model Terms	B[a]	SE[b]	SS[c]	DF[d]	*F*-Value	*P*-Value
Intercept	48.783333	1.511944	-	-	-	-
X_1	0.58375	0.925873	2.7261	1	0.3975	0.5561
X_2	-16.24125	0.925873	2110.2256	1	307.7060	<.0001*
X_3	0.2625	0.925873	0.5513	1	0.0804	0.7881
$X_1 X_2$	0.1075	1.309382	0.0462	1	0.0067	0.9378
$X_1 X_3$	1.005	1.309382	4.0401	1	0.5891	0.4774
$X_2 X_3$	-0.38	1.309382	0.5776	1	0.0842	0.7833
X_1^2	-5.032917	1.362848	93.5271	1	13.6378	0.0141*
X_2^2	-25.75292	1.362848	1448.7854	1	257.0736	<.0001*
X_3^2	-8.545417	1.362848	269.6276	1	39.3162	0.0015*

R^2, 0.97; [a]Coefficient; [b]Standard error; [c]Sum of Squares; [d]Degrees of freedom; f-values and p-values

Table 7. ANOVA result for the quadratic regression model of CO selectivity

Model Terms	B[a]	SE[b]	SS[c]	DF[d]	*F*-Value	*P*-Value
Intercept	57.35	1.019677	-	-	-	-
X_1	0.23125	0.624422	0.4278	1	0.1372	0.7263
X_2	-21.1	0.624422	3561.6800	1	1141.848	<.0001*
X_3	0.05125	0.624422	0.0210	1	0.0067	0.9378
$X_1 X_2$	0.02	0.883066	0.0016	1	0.0005	0.9828
$X_1 X_3$	0.2875	0.883066	0.3306	1	0.1060	0.7579
$X_2 X_3$	-0.385	0.883066	0.5929	1	0.1901	0.6810
X_1^2	-6.05375	0.919125	135.3153	1	43.3811	0.0012*
X_2^2	-29.09125	0.919125	3124.8031	1	1001.788	<.0001*
X_3^2	-8.26375	0.919125	252.1461	1	80.8361	0.0003*

R^2, 0.99; [a]Coefficient; [b]Standard error; [c]Sum of Squares; [d]Degrees of freedom; f-values and p-values

Table 8. Comparison between the experimental and predicted data at optimum conditions

Parameters [L/min]	Response [%]	Experimental Data [%]	Predicted Data [%] (Eqs. (17-21))	Error [%]
CH_4 = 0.19	CH_4 Conversion	79.35	80.64	1.59
CO_2 = 0.38	CO_2 Conversion	44.82	43.15	3.72
N_2 = 1.49	N_2 Conversion	3.22	3.08	4.34
	H_2 Selectivity	50.12	50.24	0.23
	CO Selectivity	58.42	57.33	1.86

Table 9. Comparison between previous studies with the current study

Production method	Feed Gas Flow Rate [L min^{-1}]			CO_2/CH_4 Ratio	Total Flow Rate [L min^{-1}]	*Specific energy [kJ L^{-1}]	Power [W]	Conversion [%]			Selectivity [%]		Refs
	CO_2	CH_4	N_2					CH_4	CO_2	N_2	H_2	CO	
Arc Jet Plasma (AJP)	2	2	16	1/1	20	0.00083	1000	50.74	35.55	NA	80.98	78.31	[40]
Cold Plasma Jet (CPJ)	3.334	5	8.334	2/3	16.667	0.0008	770	45.68	34.03	NA	78.11	85.41	[38]
Microwave reformer	1.5	0.75	NA	2/1	2.25	0.00148	2000	79.41	41.7	NA	NA	NA	[62]
Microwave pilot plant	16.67	16.67	NA	1/1	33.34	0.00415	8300	88.13	93.36	NA	75.37	69.72	[63]
Microwave plasma torch	15	15	NA	1/1	30	0.00334	6000	86.84	48.41	NA	54.61	65.92	[64]
Microwave Plasma	0.38	0.17	1.49	2/1	2.04	0.00571	700	84.91	44.40	3.37	51.31	61.17	This study

Not Available (NA)

5. Conclusions

The effect of the feed gas flow rates (CO_2, CH_4, and N_2) and their interactions on process performance to produce syngas (H_2 and CO) has been investigated by a microwave plasma reactor at atmospheric pressure. The conversions of CH_4, CO_2 and N_2 and selectivities of H_2 and CO were determined and optimised. The Behnken-Box design and response surface methodology have been used to determine the interactions of feed flow rate variables in the dry reforming of methane technology. Regression models have been developed to describe the relationships between the feed flow rate variables and reaction performance (conversions and selectivities). ANOVAs were applied to estimate a significant interaction flow rates of CO_2 with CH_4 to produce H_2 and CO via the plasma process. The results show that the CO_2 and CH_4 conversion and selectivity of H_2 and CO decrease with the increasing the gas feed flow rate. The most significant effect on process parameters and process performances was had by the flow rate of CO_2 (x_2) compared with other parameters CH_4 (x_1) and N_2 (x_3). The interactions of different process parameters have a very weak effect on CH_4, CO_2 and N_2 conversions and on H_2 and CO selectivities. The optimum coefficient of determination (R^2) of the regression equations for the CH_4, CO_2 and N_2 conversion were 0.97, 0.99 and 0.97, respectively, while those of the selectivity of H_2 and CO were 0.98 and 0.97, respectively. The optimal CH_4, CO_2 and N_2 conversion were 84.91%, 44.40% and 3.37%, respectively, and the selectivity of H_2 and CO were 51.31% and 61.17%, respectively. The optimal plasma condition was achieved when the gas feed flow rates of CH_4, CO_2 and N_2 were 0.19, 0.38, and 1.49 L min.$^{-1}$, respectively. The experimental results under the theoretical optimal conditions have explained the ability and reliability of the DoE for understanding the effect of process variables and their interaction on the process parameters and performances.

Competing financial interests

The authors declare no competing financial interests.

Acknowledgements

First of all, I would like to thank my supervisor Dr Gia Hung Pham for his patience, advice, support and encouragement during this work. The first author would like to gratefully acknowledge the Ministry of Higher Education & Scientific Research in Iraq for their sponsorship for his PhD study at Curtin University.

Nomenclature

Abbreviations

BBD	Box-Behnken Design
RSM	Response Surface Methodology
ANOVA	Analysis of Variance

Y Response

Symbol Description and units

CH_4 Methane Gas, L min^{-1}

CO_2 Carbon Dioxide Gas, L min^{-1}

N_2 Nitrogen Gas, L min^{-1}

H_2 Hydrogen Gas, L min^{-1}

CO Carbon Monoxide, L min^{-1}

Greek Characters

β Coefficient

Subscripts

β_0 Constant coefficient

β_i Coefficient for linear

x_i Initial input parameters

β_{ii} Quadratic coefficient

β_{ij} Coefficient for interactions

References

1. Khoja, A.H., M. Tahir, and N.A.S. Amin, *Dry reforming of methane using different dielectric materials and DBD plasma reactor configurations.* Energy Conversion and Management, 2017. **144**: p. 262-274.
2. Tu, X. and J.C. Whitehead, *Plasma dry reforming of methane in an atmospheric pressure AC gliding arc discharge: co-generation of syngas and carbon nanomaterials.* international journal of hydrogen energy, 2014. **39**(18): p. 9658-9669.
3. Li, L., et al., *Performance of bio-char and energy analysis on CH 4 combined reforming by CO 2 and H 2 O into syngas production with assistance of microwave.* Fuel, 2018. **215**: p. 655-664.
4. Yabe, T., et al., *Low-temperature dry reforming of methane to produce syngas in an electric field over La-doped Ni/ZrO 2 catalysts.* Fuel Processing Technology, 2017. **158**: p. 96-103.
5. Akbari-Emadabadi, S., et al., *Production of hydrogen-rich syngas using Zr modified Ca-Co bifunctional catalyst-sorbent in chemical looping steam methane reforming.* Applied Energy, 2017. **206**: p. 51-62.
6. Nawfal, M., et al., *Hydrogen production by methane steam reforming over Ru supported on Ni–Mg–Al mixed oxides prepared via hydrotalcite route.* International Journal of Hydrogen Energy, 2015. **40**(2): p. 1269-1277.

7. Figen, H.E. and S.Z. Baykara, *Effect of ruthenium addition on molybdenum catalysts for syngas production via catalytic partial oxidation of methane in a monolithic reactor.* International Journal of Hydrogen Energy, 2018. **43**(2): p. 1129-1138.
8. Peymani, M., S.M. Alavi, and M. Rezaei, *Preparation of highly active and stable nanostructured Ni/CeO 2 catalysts for syngas production by partial oxidation of methane.* International journal of hydrogen energy, 2016. **41**(15): p. 6316-6325.
9. Usman, M., W.W. Daud, and H.F. Abbas, *Dry reforming of methane: influence of process parameters—a review.* Renewable and Sustainable Energy Reviews, 2015. **45**: p. 710-744.
10. Li, L., et al., *Methane dry and mixed reforming on the mixture of bio-char and nickel-based catalyst with microwave assistance.* Journal of Analytical and Applied Pyrolysis, 2017. **125**: p. 318-327.
11. Oyama, S.T., et al., *Dry reforming of methane has no future for hydrogen production: comparison with steam reforming at high pressure in standard and membrane reactors.* international journal of hydrogen energy, 2012. **37**(13): p. 10444-10450.
12. Itkulova, S., et al., *Syngas production by bireforming of methane over Co-based alumina-supported catalysts.* Catalysis Today, 2014. **228**: p. 194-198.
13. Dry, M.E., *The fischer–tropsch process: 1950–2000.* Catalysis today, 2002. **71**(3-4): p. 227-241.
14. Czylkowski, D., et al., *Microwave plasma-based method of hydrogen production via combined steam reforming of methane.* Energy, 2016. **113**: p. 653-661.
15. Cleiren, E., et al., *Dry Reforming of Methane in a Gliding Arc Plasmatron: Towards a Better Understanding of the Plasma Chemistry.* ChemSusChem, 2017. **10**(20): p. 4025-4036.
16. Chung, W.-C. and M.-B. Chang, *Dry reforming of methane by combined spark discharge with a ferroelectric.* Energy Conversion and Management, 2016. **124**: p. 305-314.
17. Jamróz, P., W. Kordylewski, and M. Wnukowski, *Microwave plasma application in decomposition and steam reforming of model tar compounds.* Fuel Processing Technology, 2018. **169**: p. 1-14.
18. Aw, M.S., et al., *Strategies to enhance dry reforming of methane: Synthesis of ceria-zirconia/nickelecobalt catalysts by freeze-drying and NO calcination.* international journal of hydrogen energy, 2014. **39**(12636): p. e12647.
19. Snoeckx, R., et al., *Plasma-based dry reforming: improving the conversion and energy efficiency in a dielectric barrier discharge.* RSC Advances, 2015. **5**(38): p. 29799-29808.
20. Serrano-Lotina, A. and L. Daza, *Influence of the operating parameters over dry reforming of methane to syngas.* International Journal of Hydrogen Energy, 2014. **39**(8): p. 4089-4094.
21. Pakhare, D. and J. Spivey, *A review of dry (CO 2) reforming of methane over noble metal catalysts.* Chemical Society Reviews, 2014. **43**(22): p. 7813-7837.
22. Adris, A., S. Elnashaie, and R. Hughes, *A fluidized bed membrane reactor for the steam reforming of methane.* The Canadian Journal of Chemical Engineering, 1991. **69**(5): p. 1061-1070.
23. Ashcroft, A., et al., *Partial oxidation of methane to synthesis gas using carbon dioxide.* Nature, 1991. **352**(6332): p. 225-226.
24. Zhang, J.-Q., et al., *Oxidative coupling and reforming of methane with carbon dioxide using a pulsed microwave plasma under atmospheric pressure.* Energy & fuels, 2003. **17**(1): p. 54-59.
25. Jiang, T., et al., *Plasma methane conversion using dielectric-barrier discharges with zeolite A.* Catalysis Today, 2002. **72**(3): p. 229-235.

26. Ayodele, B.V., et al., *Modelling and optimization of syngas production by methane dry reforming over samarium oxide supported cobalt catalyst: response surface methodology and artificial neural networks approach.* Clean Technologies and Environmental Policy, 2017. **19**(4): p. 1181-1193.
27. Mei, D., et al., *Optimization of CO2 conversion in a cylindrical dielectric barrier discharge reactor using design of experiments.* Plasma Processes and Polymers, 2016. **13**(5): p. 544-556.
28. De Bie, C., J. van Dijk, and A. Bogaerts, *The dominant pathways for the conversion of methane into oxygenates and syngas in an atmospheric pressure dielectric barrier discharge.* The Journal of Physical Chemistry C, 2015. **119**(39): p. 22331-22350.
29. Senseni, A.Z., et al., *A comparative study of experimental investigation and response surface optimization of steam reforming of glycerol over nickel nano-catalysts.* International Journal of Hydrogen Energy, 2016. **41**(24): p. 10178-10192.
30. Hafizi, A., M. Rahimpour, and S. Hassanajili, *Hydrogen production by chemical looping steam reforming of methane over Mg promoted iron oxygen carrier: Optimization using design of experiments.* Journal of the Taiwan Institute of Chemical Engineers, 2016. **62**: p. 140-149.
31. Abedini, F., et al., *Design and optimization of new La1− xCexNi1− yFeyO3 (x, y= 0–0.4) nano catalysts in dry reforming of methane.* International Journal of Green Energy, 2017: p. 1-8.
32. Montgomery, D.C., *Design and analysis of experiments*. 2017: John Wiley & Sons.
33. Wu, L., et al., *Application of the Box–Behnken design to the optimization of process parameters in foam cup molding.* Expert Systems with Applications, 2012. **39**(9): p. 8059-8065.
34. Challiwala, M.S., et al., *A Process Integration Approach to the Optimization of CO2 Utilization via Tri-Reforming of Methane*, in *Computer Aided Chemical Engineering*. 2017, Elsevier. p. 1993-1998.
35. Ramachandran, C., V. Balasubramanian, and P. Ananthapadmanabhan, *Multiobjective optimization of atmospheric plasma spray process parameters to deposit yttria-stabilized zirconia coatings using response surface methodology.* Journal of thermal spray technology, 2011. **20**(3): p. 590-607.
36. Sidik, S., et al., *CO 2 reforming of CH 4 over Ni–Co/MSN for syngas production: Role of Co as a binder and optimization using RSM.* Chemical Engineering Journal, 2016. **295**: p. 1-10.
37. Abbasi, M., et al., *Modeling and optimization of synthesis parameters in nanostructure La 1− xBaxNi 1− yCuyO 3 catalysts used in the reforming of methane with CO 2.* Journal of the Taiwan Institute of Chemical Engineers, 2017. **74**: p. 187-195.
38. Long, H., et al., *CO 2 reforming of CH 4 by combination of cold plasma jet and Ni/γ-Al 2 O 3 catalyst.* international journal of hydrogen energy, 2008. **33**(20): p. 5510-5515.
39. Li, X.S., et al., *Carbon dioxide reforming of methane in kilohertz spark-discharge plasma at atmospheric pressure.* AIChE Journal, 2011. **57**(10): p. 2854-2860.
40. Hwang, N., Y.-H. Song, and M.S. Cha, *Efficient Use of $\hbox {CO}_ {2} $ Reforming of Methane With an Arc-Jet Plasma.* IEEE Transactions on Plasma Science, 2010. **38**(12): p. 3291-3299.
41. Tao, X., et al., *CO 2 reforming of CH 4 by combination of thermal plasma and catalyst.* International Journal of Hydrogen Energy, 2008. **33**(4): p. 1262-1265.
42. Yanpeng, S., et al., *Carbon dioxide reforming of methane to syngas by thermal plasma.* Plasma Science and Technology, 2012. **14**(3): p. 252.
43. Indarto, A., et al., *Effect of additive gases on methane conversion using gliding arc discharge.* Energy, 2006. **31**(14): p. 2986-2995.

44. Zhu, B., et al., *Pressurization effect on dry reforming of biogas in kilohertz spark-discharge plasma.* international journal of hydrogen energy, 2012. **37**(6): p. 4945-4954.
45. Xu, Y., et al., *CO 2 reforming of CH 4 by synergies of binode thermal plasma and catalysts.* international journal of hydrogen energy, 2013. **38**(3): p. 1384-1390.
46. Lieberman, M.A. and A.J. Lichtenberg, *Principles of plasma discharges and materials processing*. 2005: John Wiley & Sons.
47. Pei, X., et al., *Large-volume N2 plasma induced by electron beam at high pressure.* IEEE Trans. Plasma Sci, 2013. **41**(3): p. 494-497.
48. Conrads, H. and M. Schmidt, *Plasma generation and plasma sources.* Plasma Sources Science and Technology, 2000. **9**(4): p. 441.
49. Schmidt, M., et al., *Device for producing and investigating an electron beam plasma discharge.* Beiträge aus der Plasmaphysik, 1982. **22**(5): p. 435-441.
50. Meger, R., et al. *Beam Generated Plasmas for Large Area Materials Processing*. in *APS Annual Gaseous Electronics Meeting Abstracts*. 1999.
51. Wnukowski, M. and P. Jamróz, *Microwave plasma treatment of simulated biomass syngas: Interactions between the permanent syngas compounds and their influence on the model tar compound conversion.* Fuel Processing Technology, 2018. **173**: p. 229-242.
52. Alketife, A.M., S. Judd, and H. Znad, *Synergistic effects and optimization of nitrogen and phosphorus concentrations on the growth and nutrient uptake of a freshwater Chlorella vulgaris.* Environmental technology, 2017. **38**(1): p. 94-102.
53. El Hassani, K., B. Beakou, and A. Anouar, *Analysis of adsorption of azo dye onto NiAl-CO3 using Box-Behnken design approach and desirability function.* 2018.
54. Mallieswaran, K., R. Padmanabhan, and V. Balasubramanian, *Friction stir welding parameters optimization for tailored welded blank sheets of AA1100 with AA6061 dissimilar alloy using response surface methodology.* Advances in Materials and Processing Technologies, 2018: p. 1-16.
55. Moore, J.W. and C.L. Stanitski, *Chemistry: The molecular science*. 2014: Cengage Learning.
56. Rayne, S., *Thermal carbon dioxide splitting: A summary of the peer-reviewed scientific literature.* 2008.
57. Volynets, A., D. Lopaev, and N. Popov. *Mechanism of N2 dissociation and kinetics of N (4S) atoms in pure nitrogen plasma*. in *Journal of Physics: Conference Series*. 2016. IOP Publishing.
58. Timmermans, E., et al., *The behavior of molecules in microwave-induced plasmas studied by optical emission spectroscopy. 1. Plasmas at atmospheric pressure.* Spectrochimica Acta Part B: Atomic Spectroscopy, 1998. **53**(11): p. 1553-1566.
59. Allah, Z.A. and J.C. Whitehead, *Plasma-catalytic dry reforming of methane in an atmospheric pressure AC gliding arc discharge.* Catalysis Today, 2015. **256**: p. 76-79.
60. Rieks, M., et al., *Experimental study of methane dry reforming in an electrically heated reactor.* International Journal of Hydrogen Energy, 2015. **40**(46): p. 15940-15951.
61. Ehrgott, M., *Multicriteria optimization*. Vol. 491. 2005: Springer Science & Business Media.
62. Chun, Y.N. and M.S. Lim, *Produced Gas Conversion of Microwave Carbon Receptor Reforming.* World Academy of Science, Engineering and Technology, International Journal of Environmental, Chemical, Ecological, Geological and Geophysical Engineering. **12**(1): p. 17-23.

63. Fidalgo, B. and J. Menéndez, *Study of energy consumption in a laboratory pilot plant for the microwave-assisted CO2 reforming of CH4.* Fuel processing technology, 2012. **95**: p. 55-61.
64. Chun, S.M., Y.C. Hong, and D.H. Choi, *Reforming of methane to syngas in a microwave plasma torch at atmospheric pressure.* Journal of CO2 Utilization, 2017. **19**: p. 221-229.